PASJ: Publ. Astron. Soc. Japan **63**, 971–978, 2011 October 25

Detection of Acoustic/Infrasonic/Seismic Waves Generated by Hypersonic Re-Entry of the HAYABUSA Capsule and Fragmented Parts of the Spacecraft

Masa-yuki YAMAMOTO,[1] Yoshiaki ISHIHARA,[2] Yoshihiro HIRAMATSU,[3] Kazuki KITAMURA,[1] Masayoshi UEDA,[4] Yasuo SHIBA,[4] Muneyoshi FURUMOTO,[5] and Kazuhisa FUJITA[6]

[1]*Kochi University of Technology, 185 Miyanokuchi, Tosayamada-cho, Kami, Kochi 782-8502*
yamamoto.masa-yuki@kochi-tech.ac.jp
[2]*National Astronomical Observatory of Japan, 2-12 Hoshigaoka-cho, Mizusawa-ku, Oshu, Iwate 023-0861*
[3]*Kanazawa University, Kakuma, Kanazawa, Ishikawa 920-1192*
[4]*Nippon Meteor Society, 43-2 Asuka, Habikino, Osaka 583-0842*
[5]*Nagoya University, Furo-cho, Chikusa-ku, Nagoya 464-8602*
[6]*Japan Aerospace Exploration Agency, 7-44-1 Shindaiji-higashimachi, Chofu, Tokyo 182-8522*

(Received 2011 March 31; accepted 2011 August 9)

Abstract

Acoustic/infrasonic/seismic waves were observed during the re-entry of the Japanese asteroid explorer "HAYABUSA" at 6 ground sites in Woomera, Australia, on 2010 June 13. Overpressure values of infrasound waves were detected at 3 ground sites in a range from 1.3 Pa, 1.0 Pa, and 0.7 Pa with each distance of 36.9 km, 54.9 km, and 67.8 km, respectively, apart from the SRC trajectory. Seismic waveforms through air-to-ground coupling processes were also detected at 6 sites, showing a one-to-one correspondence to infrasound waves at all simultaneous observation sites. Audible sound up to 1 kHz was recorded at one site with a distance of 67.8 km. The mother spacecraft was fragmented from 75 km down to 38 km with a few explosive enhancements of emissions. A persistent train of HAYABUSA re-entry was confirmed at an altitude range of between 92 km down to 82 km for about 3 minutes. Light curves of 136 fragmented parts of the spacecraft were analyzed in detail based on video observations taken at multiple ground sites, being classified into three types of fragmentations, i.e., melting, explosive, and re-fragmented types. In a comparison between infrasonic waves and video-image analyses, regarding the generation of sonic-boom type shock waves by hypersonically moving artificial meteors, both the sample return capsule and fragmented parts of the mother spacecraft, at an altitude of 40 ± 1 km were confirmed with a one-to-one correspondence with each other.

Key words: Earth, atmosphere — meteors, artificial — space vehicles

1. Introduction

In order to obtain sample materials from the asteroid Itokawa (25143), the Japanese spacecraft HAYABUSA cruised in interplanetary space starting in 2003. After its successful exploration and landing twice on Itokawa in 2005 (e.g., Fujiwara et al. 2006), HAYABUSA traveled for 5 more years back to the Earth, landing at Woomera, Australia on 2010 June 13. In the final phase of the HAYABUSA return, a SRC (sample return capsule) reentered into the Earth's atmosphere and successfully landed. Because of partial failure in attitude control, the mother S/C (spacecraft) also reentered at almost the same time. The SRC was released from S/C 3 hours prior to the re-entry, and two bodies were within a distant/temporal separation of only 2 km/0.17 s. Re-entry of the spacecraft directly from interplanetary space with an incident speed of 12 km s^{-1} or larger is very rare, and the HAYABUSA re-entry was the third opportunity to investigate the interaction between artificial materials from an interplanetary orbit and the Earth's upper atmosphere during a controlled re-entry, since the end of the US Apollo program (Yamaguchi et al. 2011).

Shock waves generated by hypersonic entry of meteors and meteorites in the upper atmosphere have been reported since Whipple et al. (1930). Seismic signals can also be generated by fireballs with an air-to-ground coupling process (e.g., Ishihara et al. 2003). Shock waves can be propagated in the atmosphere as audible and infrasonic sound waves. Due to its long-propagation ability, the observation of infrasonic waves is known as a remote sensing method. Recently, infrasonic waves are used to monitor and determine a wave source generated by artificial explosions, such as nuclear-weapons tests in the context of CTBTO (Comprehensive Nuclear-Test-Ban Treaty Organization), applied to scientific approaches of meteor physics and artificial re-entry analyses (Brown et al. 2002; ReVelle et al. 2005; Spurný et al. 2010).

Array observations of infrasound waves are required to examine the accuracy of the incident wave vector by using any opportunity of known infrasonic wave sources. As an artificial meteor, infrasonic waves excited by a re-entry of Stardust SRC were investigated (Edwards et al. 2007). The re-entry of HAYABUSA is important to study infrasound propagation from the thermosphere to the ground. Still images and video observations of the HAYABUSA re-entry are also important to study the fragmentation process of the spacecraft. Here, we report on preliminary results of infrasound and seismic observations of the HAYABUSA re-entry as well as optical observations.

Table 1. Sensors and cameras deployed to GOS sites (only concerns of this paper).

Sensor type	Site name	Maker, specification, number of pieces
High-sensitivity video camera	GOS2	Watec, WAT-100N (1.6–3.4 mm lens)
	GOS2	Watec, WAT-902H ULTIMATE (2.9–8 mm lens) ×2
	GOS3	Watec, WAT-902H ULTIMATE (2.9–8 mm lens) ×2
	GOS4	Watec, WAT-902H ULTIMATE (2.9–8 mm lens) ×2
Digital camera	GOS2	Nikon, D3 (28 mm F/2 lens)
Digital camera (spectroscopy)	GOS2	Nikon, D700 (35 mm F/2) & Shimadzu, grating (600 l/mm)
Infrasound sensor	GOS2	Chaparral physics, Model-2
	GOS2A	Chaparral physics, Model-2.5 ×3
	GOS2B	Chaparral physics, Model-2
Microphone (audible)	GOS2	Loas, MMP-04; OLYMPUS, Voice-Trek V-40 (recorder)
Seismometer (vertical)	GOS2	Hakusan, SG820 ×5
	GOS2A	Hakusan, SG820 ×6
	GOS2B	Hakusan, SG820 ×4
	GOS2B-sub1	Hakusan, SG820
	GOS2B-sub2	Hakusan, SG820
	GOS2B-sub3	Hakusan, SG820
Seismometer (three-components)	GOS2	Sercel (MARK PRODUCT), L-28-3D
	GOS2A	Sercel (MARK PRODUCT), L-28-3D

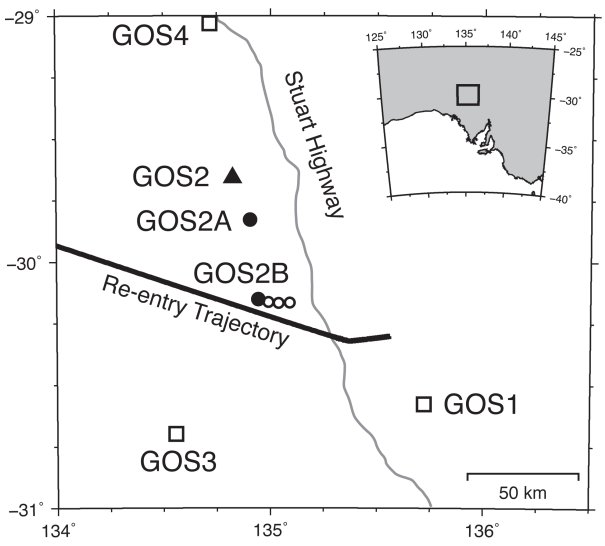

Fig. 1. Location of ground observation sites and the HAYABUSA trajectory. GOS1, GOS2, GOS3, and GOS4 were optical observation sites. At GOS2, acoustic/infrasound/seismic array observations were carried out. GOS2A and GOS2B were automatic observation sites for infrasonic/seismic sensor arrays. Open circles indicate 3 subsidiary stations of GOS2B-sub1, -sub2, and -sub3.

2. Observation

As a part of JAXA's ground-based optical observations of the HAYABUSA re-entry (Fujita et al. 2011), we operated a combined observation of infrasonic and seismic waves in the WPA (Woomera Prohibited Area), Australia. As shown in figure 1, infrasound observations were carried out at 3 sites (GOS2, GOS2A, and GOS2B); also, seismic waves were measured there, and at 3 more sites (GOS2B-sub1 to -sub3). In order to obtain the incident angle, i.e., the azimuth and elevation of shock waves, array observations were conducted at the former 3 sites. We used Chaparral physics Model-2 and Model-2.5 infrasound sensors, whose detectable frequency range was from 0.1 Hz to 200 Hz with a flat response within 3 dB; 5 infrasound sensors in total were installed at the sites GOS2, GOS2A, and GOS2B in the WPA, with having each slant range of about 67.8 km, 54.9 km, and 36.9 km, respectively, apart from the SRC trajectory. The sites GOS2B-sub1 to -sub3 were located on a line almost parallel to the re-entry trajectory. Two three-component (one vertical and two horizontal) velocity seismometers were deployed only at GOS2 and GOS2A, whereas 18 vertical-component velocity seismometers were put at all sites. Optical observations were carried out at GOS1, GOS2, GOS3, and GOS4, through collaboration with the other team members (Fujita et al. 2011). Here, we used high-sensitivity video movies recorded at GOS2, GOS3, and GOS4 (Ueda et al. 2011). The sensors and cameras used in this study are summarized in table 1. Hakusan LS-7000 and LS-8200SD data loggers were used to record 100 Hz and 125 Hz samplings (at a sampling mode of each logger higher than 50 Hz) of infrasound/seismic data, respectively, with the accuracy of timing being within 1 ms using GPS.

3. Results

During the HAYABUSA re-entry, SRC and S/C appeared in the sky as one point light source at 101 km altitude taken by WAT-902H video movies (Ueda et al. 2011). The most faint luminescence was found at 110 km altitude by a still image with 1 s exposure and ISO = 6400 taken by a Nikon D3. With increasing luminescence emission during its descent, two explosive enhancements were observed at 68 km (bluish flash) and 58 km (reddish flash), respectively. After the peak heat altitude of the SRC (about 57.7 km in prediction by JAXA capsule

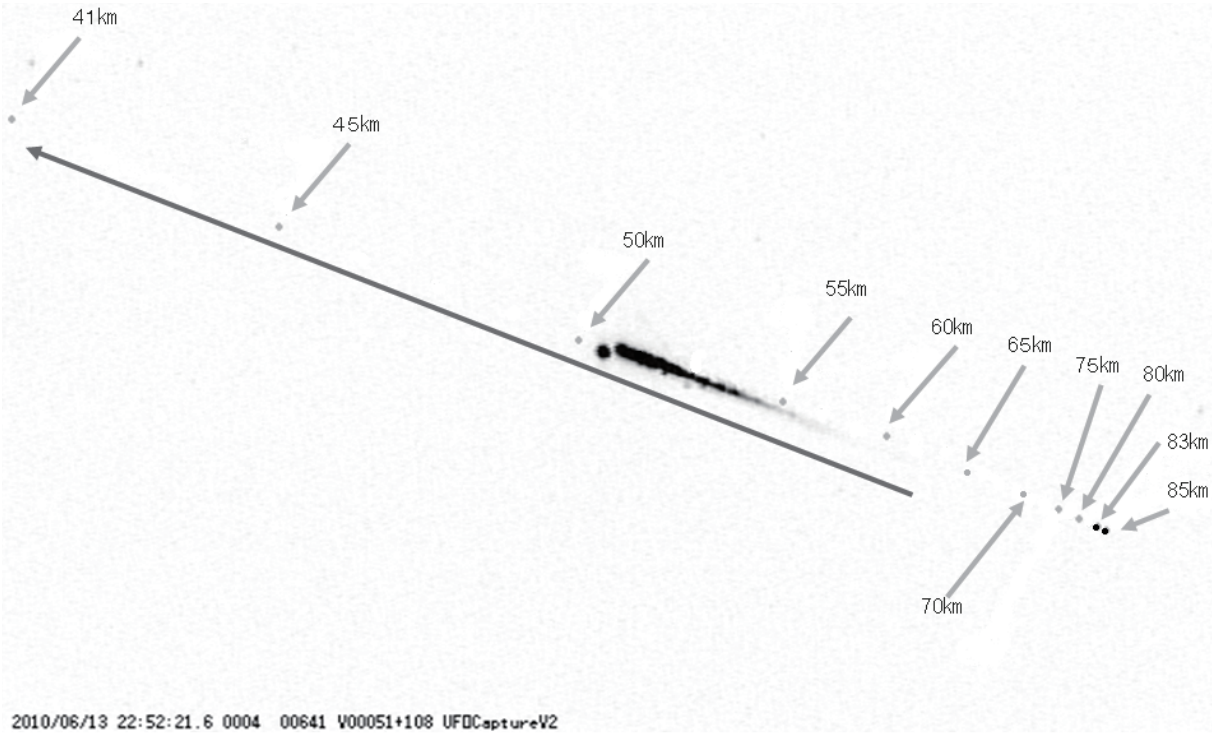

Fig. 2. Fragmentation process captured on snapshot images. A snapshot taken at GOS2 by a high-sensitivity CCD video camera, WAT-902H Ultimate, at 13:52:21.6 UT shown with a scale of altitude.

resumption team, 2010), the emission can be determined as two separate points of the forming SRC and the following S/C with a separation distance of about 2 km. In an altitude range of from 75 km down to 38 km, complicating fragmentation of S/C was clearly detected by all video cameras at GOS sites (figure 2). In the cases of meteorite falls, after having significant aerodynamic deceleration, meteorite bodies usually show a "dark flight" period without any visible emission from the bodies due to low temperature on the surfaces. Light curves of the SRC and S/C are shown by Watanabe et al. (2011) and Ueda et al. (2011), indicating that the transient altitude to "dark flight" of the SRC was at about 36 km. Faint luminescence as a persistent meteor train was confirmed in successive images taken by digital cameras at an altitude range of from 92 km down to 82 km for about 3 minutes (see figure 10 of Fujita et al. 2011). Infrasonic observations of the shock waves generated by the hypersonic SRC re-entry were successfully detected as an N-type wavelet at all 3 sites of GOS2, GOS2A, and GOS2B, followed with a few enhancements of pressure waves (figure 3). We here convert the ground-velocity waveforms recorded by the seismometer to the displacement using time integration. In figure 3, impulsive signals are found in waveform data recorded by an infrasound sensor and a three-component seismometer. The amplitude of the vertical component is larger than those of the horizontal ones, showing effective air-to-ground couplings in the case of an almost vertical incident beam angle. Seismograms observed by 18 sensors at all 6 sites are shown in detail by Ishihara et al. (2011). Moreover, audible sound was heard by all observers at GOS2. Band-pass filtered waveforms of 20–45 Hz confirm the sound as being a few impulsive signals detected by a microphone as well as infrasound sensors at GOS2 (figure 4). The sound was also recorded by the other team near at the GOS3 site (Akita et al. private communication, 2010). Seismometers deployed at GOS2, GOS2A, GOS2B, and GOS2B-sub1 to -sub3 observed impulsive signals at the corresponding arrival times of infrasonic waves. The absolute value of the pressure wave generated by the HAYABUSA SRC was about 1.3, 1.0, and 0.7 Pa (as overpressure level of positive sign) at the sites of GOS2B, GOS2A, and GOS2, respectively, with respect to each slant range of 36.9 km, 54.9 km, and 67.8 km.

4. Discussion

The fragmentation process of the HAYABUSA S/C was carefully analyzed based on 7 video movies taken at GOS2, GOS3, and GOS4. In figure 5, light curves of 136 fragmented parts of the HAYABUSA S/C are shown in detail, whereas figure 6 shows successive snapshots during the final part of the fragmentation of S/C. The fragmentation process was extremely complicated. We can, however, classify it into 3 types. Figure 5a shows simple descending curves (39 samples), figure 5b, enhancements at the final stage of the emissions (21), and figure 5c re-fragmented complicatedly into several parts (76). Note that more close-up images taken by Abe et al. (2011) show over 300 fragmented parts, implying that the fragmentation was finally disintegrated into pieces. From these light curves, we classified them into melting type (figure 5a), explosive type (figure 5b), and re-fragmented type (figure 5c), respectively. It can be understood as depending on

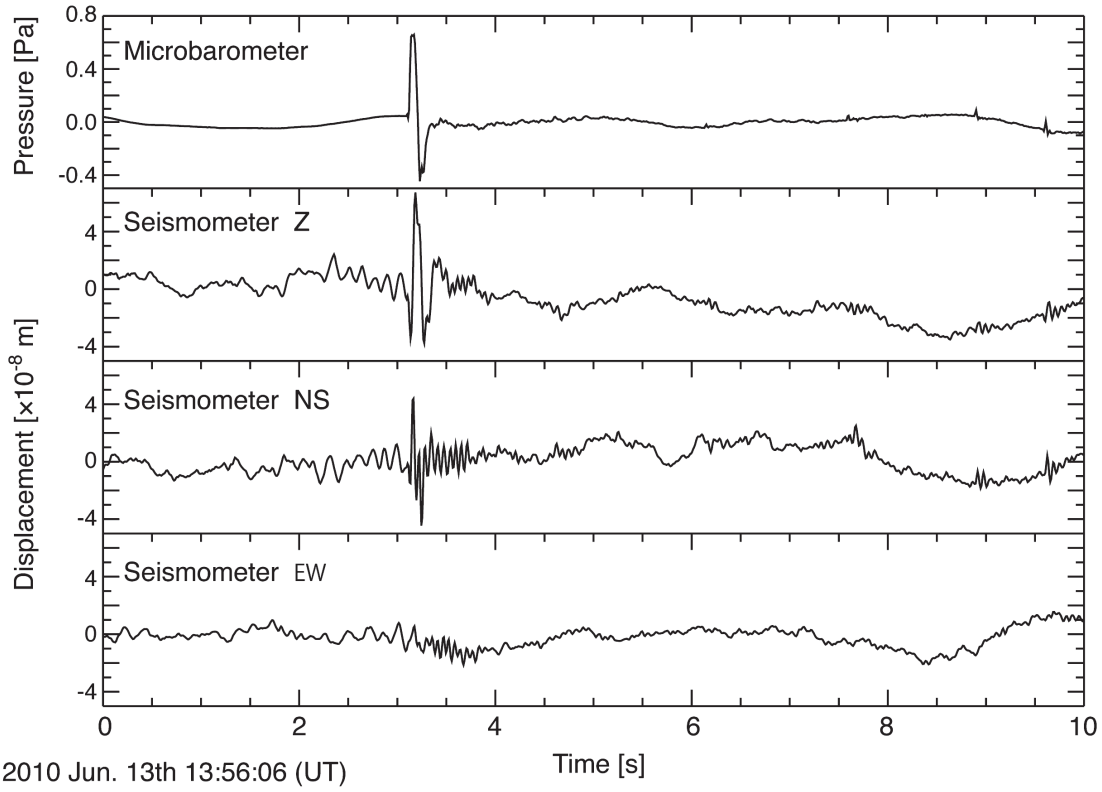

Fig. 3. Waveforms of an infrasound sensor and a three-component seismometer at GOS2. The waveforms of the seismometer were converted from velocity to displacement by the time integral.

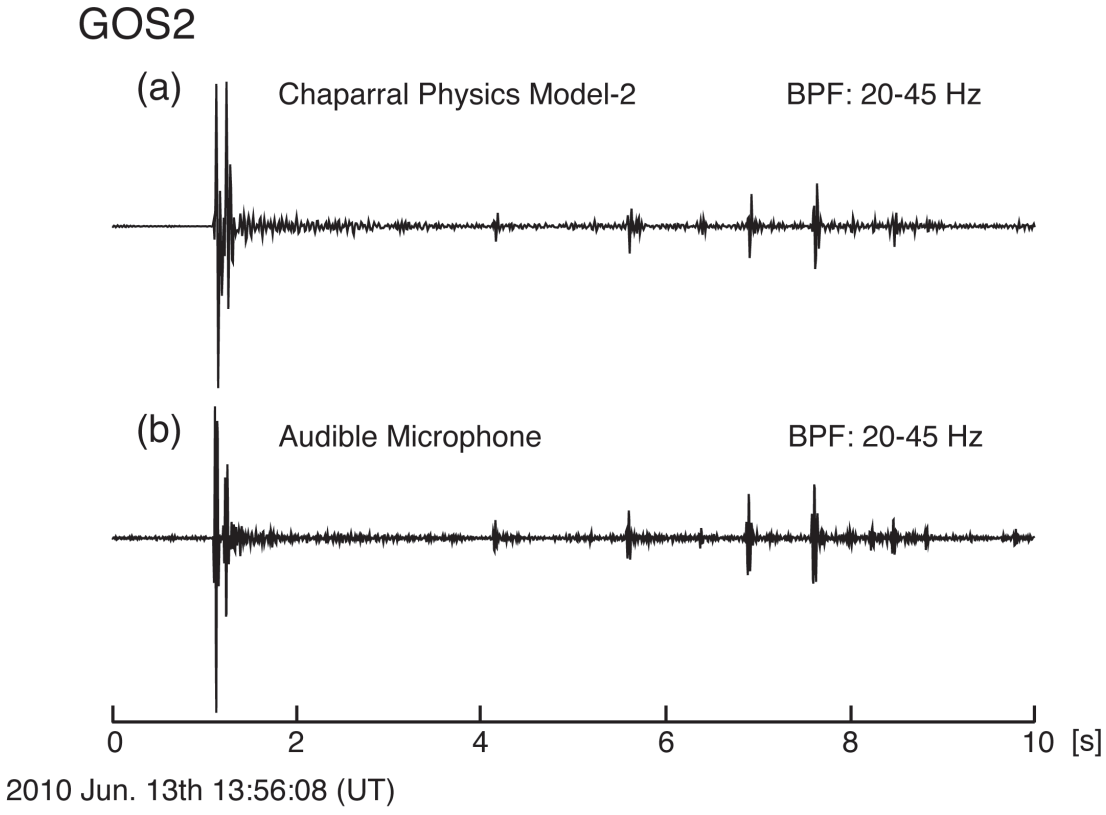

Fig. 4. Impulsive shock wave and multiple weak signals detected by audible/infrasound sensors. (A band-pass filter between 20 to 45 Hz was applied to these signals.)

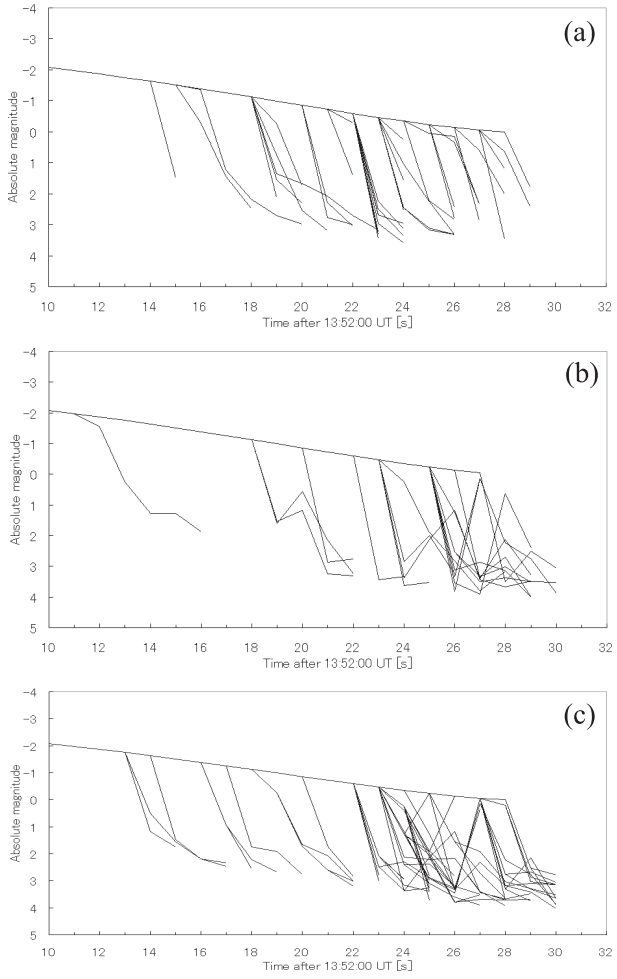

Fig. 5. Fragmentation process of HAYABUSA S/C derived from video movies. Light curves of 136 fragmented parts of HAYABUSA S/C classified into (a) melting, (b) explosive, and (c) re-fragmented types (converted to absolute magnitude at a fixed distance of 100 km). Note that the main slope from which the fragments branch off in each panel is due to the saturation level of the HAYABUSA S/C taken by the high-sensitivity camera.

the characteristics of the corresponding components of the S/C.

A statistical study by Watanabe et al. (2011) shows considerably small population indices of the fragmented parts of S/C compared with fragmentation of the natural materials. Even in the cases of the fragmented type, several fragmented parts can be pursued as point sources. Both analyses show the fragmentation process for considerably rigid "artificial" items. A few explosive enhancements were recorded in detailed light curves of the S/C shown in Ueda et al. (2011). In our analyses, the most drastic fragmentation was found at the same time of the brightest enhancement, implying that the fragmentations were caused mostly by explosive enhancement events. However, the SRC shows a gradual time trend of the illumination with a long ablated tail, having a peak brightness of -5 magnitude at an altitude of 43 km (Ueda et al. 2011), showing successful heat shield control by the TPA (thermal protection ablator) (Fujita et al. 2011).

A persistent train by the HAYABUSA re-entry shows the existence of interaction between ablated or fragmented artificial materials and the upper-atmosphere components. The center of the luminescence was higher than the SRC peak heat altitude. Due to the same luminescence observed just after the Stardust re-entry over Utah on 2006 January 15 (Abe et al. 2006), it was expected to see a persistent train of HAYABUSA, so a digital camera, Nikon D700, was deployed with a Shimadzu 600 lines mm^{-1} transparent grating for spectroscopy of the persistent train of HAYABUSA re-entry; however, it was unfortunately too faint to catch any specific line or band features of the luminescence. Spectroscopic results of SRC and S/C, themselves, shown by Abe et al. (2011), imply possible components of the illuminative interaction. The altitude range of the persistent train of HAYABUSA (92 km to 82 km) and Stardust cases were slightly lower than the statistical altitude range of natural persistent trains by bright Leonids and Orionids meteors (Yamamoto et al. 2005), probably because of the lower beginning altitude of the ablation of SRC and fragmented S/C with respect to the natural meteor cases.

Shock waves were clearly detected at all infrasound sites. From the results obtained at the GOS2 site, a 0.7 Pa pressure wave was detected at 13:56:09.1 UT after propagating for 216 s, corresponding to about 67.8 km distance (slant range) from a Mach cone of a sonic-boom type shock wave at an altitude of 40.6 km on the HAYABUSA SRC trajectory, generated by SRC passing there at 13:52:33 UT. Precise analyses of the pressure waves with propagation conditions in the atmosphere and the elastic media will be shown based on the arrayed infrasound/seismic sensors (Ishihara et al. 2011). Seismic signals were also detected at all seismometer sites as well, showing evidence of air-to-ground coupling at the WPA sites. Clear one-to-one correspondence was found between infrasound and seismic data at 13:56:09.1 UT for about 1 s during an N-type shock event as well as the following 4 tiny shocks at 13:56:12.3 UT, 13:56:13.7 UT, 13:56:14.9 UT, and 13:56:15.6 UT in a detailed comparison (figure 4). Here, the period of the N-type shock wave was briefly investigated, comparing with Genesis and Stardust results. Figure 4 of ReVelle et al. (2005) shows 0.4 s of the clear N-type shock by a 1.52 m diameter SRC of Genesis and figure 4 of Edwards et al. (2007) shows 0.2 s of N-type shock with small oscillations for a few seconds by a 0.811 m diameter SRC of Stardust. Figure 4 of this paper shows a 0.12 s N-type shock wave by 0.4 m HAYABUSA SRC. They are almost proportional to the scale size of the SRC.

Multiple audible sound signals detected at GOS2 were not so much expected; however, a supplementary equipped microphone clearly recorded the sound signal, being proved by a band-pass filtered analysis, shown in figure 4. Spectral analysis showed that sound up to a maximum frequency of 1 kHz was detected during the various arrivals. In figure 4, a few following pressure-wave signals can be seen following the arrival of the main shock front. They were also audible at GOS2. In the final stage of the fragmentation process of the S/C, three clear and a few faint point sources can be identified on successive images in figure 6.

Based on these images, the delay time between the passage of SRC and those of four parts was analyzed for each

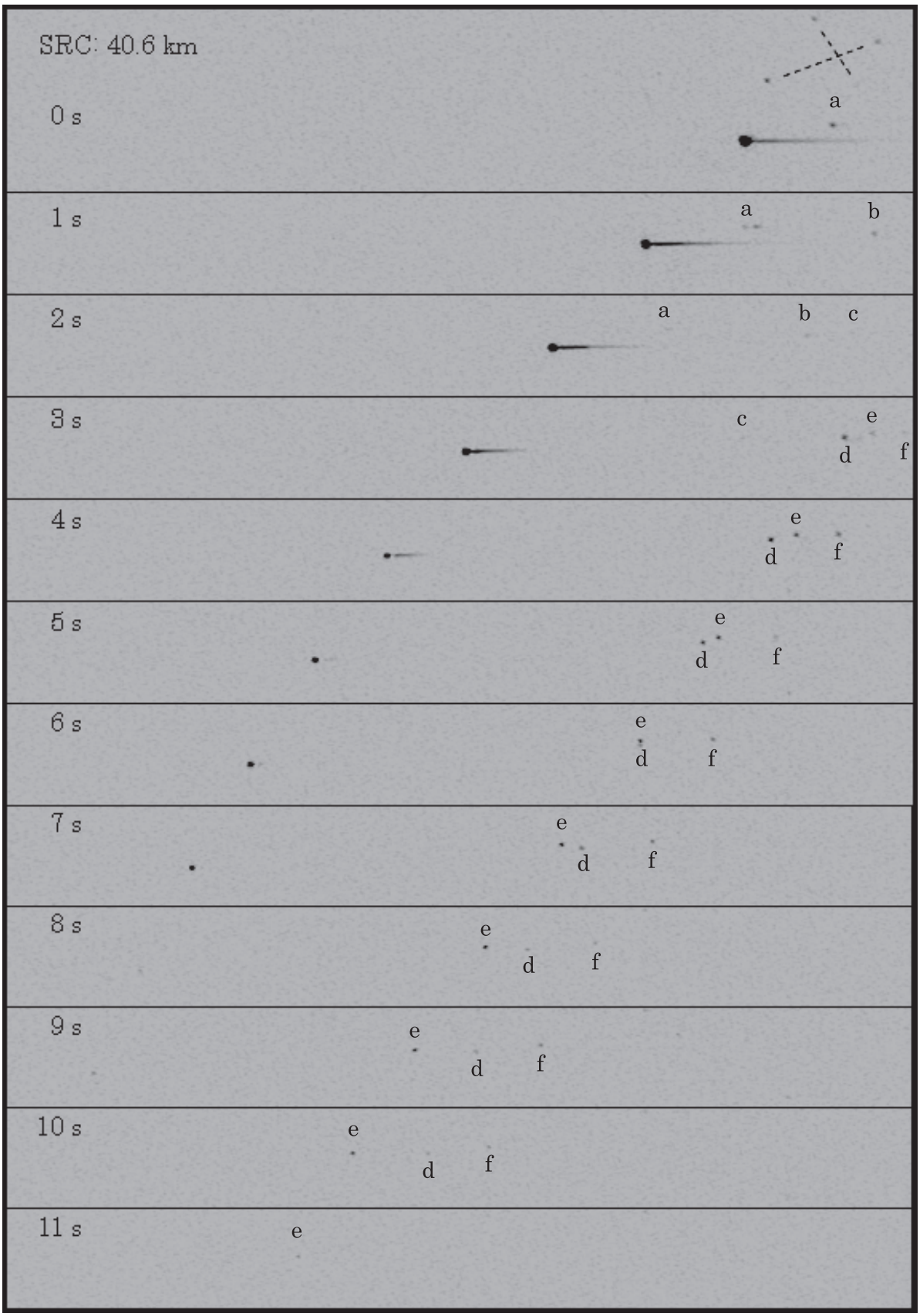

Fig. 6. Fragmentation process captured on snapshots by a WAT-902H video movie observed at GOS2 with 1 s intervals, showing the final stage of illuminative flights of SRC and fragmented parts.

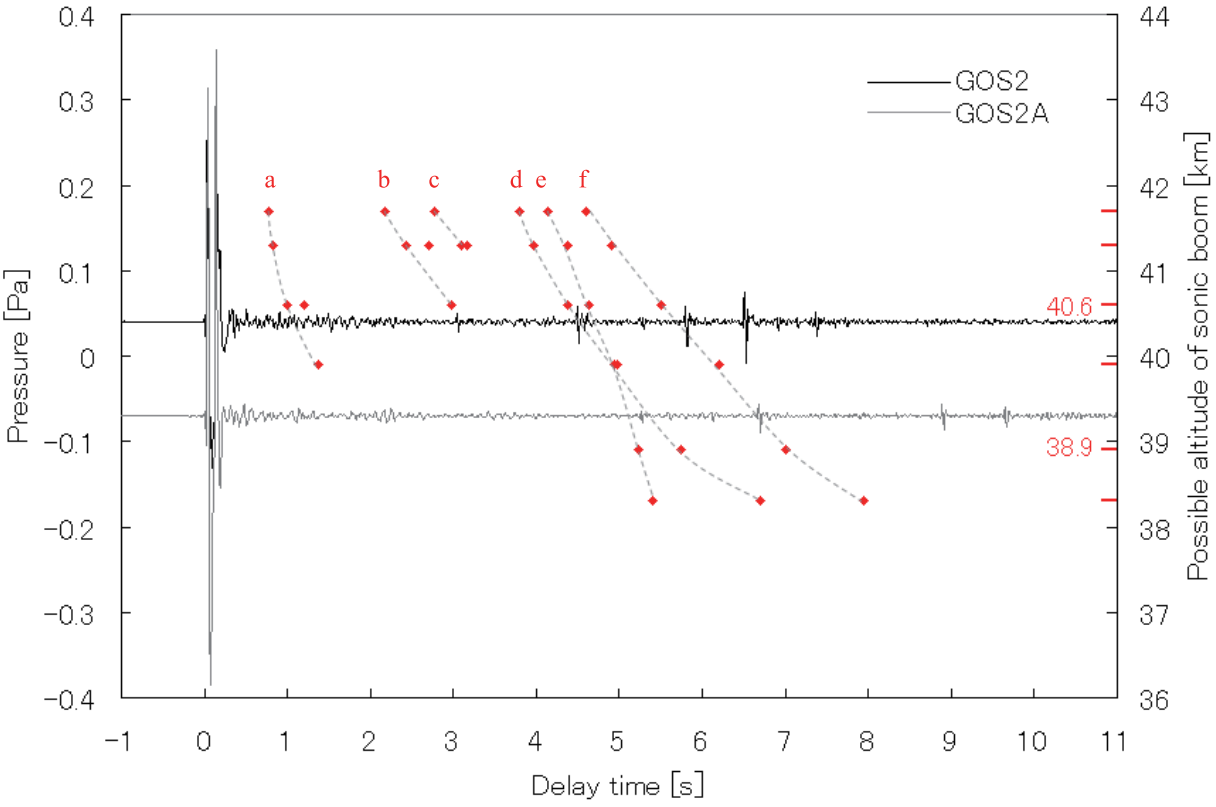

Fig. 7. Delay time between the SRC passing time and that of fragmented items at each altitude (red dots) in comparison with infrasound signals observed at GOS2 and GOS2A. Delays were measured from snapshots at 6 corresponding altitudes shown in right axis. Infrasound signals are shifted to be the best fit, namely, possible altitudes of multiple sonic-boom-type sources at 40.4 km and 39.3 km for GOS2 and GOS2A data, respectively, while the infrasound sources were roughly estimated at 40.6 km and 38.9 km, respectively.

sonic-boom type source. Figure 7 shows a comparison between the delays measured at each altitude and the detected infrasound signals at GOS2 and GOS2A, respectively. It is considered that the shock waves detected at GOS2 came from sonic-boom sources at 40.6 km altitude, whereas those detected at GOS2A were from sonic-boom sources at 38.9 km. Based on the delay time at 40.6 km altitude, each delay time of 1.0 s, 1.2 s, 3.0 s, 4.4 s, 4.6 s, and 5.5 s was likely to be considered to correspond to a small shock wave of an infrasound trend at GOS2 (see figure 7 and compare the GOS2 infrasound signal with the 6 red points, a to f, corresponding to the same symbols in figure 6). As for the 38.9 km case, time delays of 5.2 s, 5.7 s, and 7.0 s also corresponded to small shock waves. Delays of 5.3 s, 6.5 s, and 7.4 s for the GOS2 case as well as delays of 6.1 s, 8.9 s, and 9.7 s for the GOS2A case cannot be identified on images, implying that a few more "dark flight" items existed at the corresponding altitudes. In some cases, a fragmented item shows passing with the other items, implying there existed fast-small or slow-big flight parts with an advantage for pressure wave generation at lower altitudes. From the ratio between these small shock waves and the strongest shock wave by the SRC with 0.4 m diameter, the corresponding items as fragmented characteristics of HAYABUSA S/C seem to be totally banished in the atmosphere. No debris was confirmed around the SRC landing area in the WPA. The shock wave detected at GOS2B shows only the strongest one, suggesting that the pressure wave was generated by SRC at 36.5 km altitude, and whether the two explosive fragmentations could also be shock-wave sources is to be analyzed in following papers.

5. Conclusions

On 2010 June 13, during the HAYABUSA re-entry, ground based observations by optical, infrasound, and seismic sensors were carried out in WPA, Australia. The re-entry of the HAYABUSA S/C and SRC represents only the third opportunity to observe and study a hypersonic re-entry of an artificial body directly from interplanetary space with an initial velocity of $12.1 \pm 0.3\,\mathrm{km\,s^{-1}}$, since the end of the Apollo era. The S/C fragmentation process, clearly observed by multiple video movies, reveals precise light curves of 136 fragmented parts, resulting in a classification into 3 types, i.e., melting, explosive, and re-fragmented types, possibly depending on the artificial structure of the S/C. Impulsive infrasound signals with an intensity of about 1.0 Pa were detected at 3 sites with 1 arrayed observation. Simultaneously, 18 seismometers at 6 sites also detected impulsive signals. Corresponding to the infrasound signal, the audible signal up to 1 kHz was also recorded at 1 site with a distance of 67.8 km from a 40.6 km altitude point of the HAYABUSA trajectory. Following the shock front, multiple signals of weak audible/infrasonic/seismic waves were detected. They can be explained by multiple fragmented parts that reentered into 40 km altitude or lower with some delay time from the passage of SRC.

The authors would like to express sincere appreciation to the JAXA/ISAS HAYABUSA science team and the JAXA capsule resumption team for giving them permission to join the HAYABUSA re-entry observation. They are also grateful for assistance of the Australian government concerning authorization of their research activities in WPA. Vertical seismometers with data loggers were provided by Disaster Prevention Research Institute, Kyoto University (H. Katao). A digital camera Nikon D3 was provided by M. Toda (Nippon Meteor Society). The authors express their gratitude for fruitful discussions with anonymous referees to improve this paper. A part of this study is supported by the Ministry of Education, Sports, Culture, Science and Tecknology, Grant-in-Aid for Scientific Research (KAKENHI) (B), Field Research in Abroad, 22403005, 2010 (PI: Y.H.).

References

Abe, S., et al. 2011, PASJ, 63, 1011

Abe, S., Yamamoto, M.-Y., Yano, H., Ebizuka, N., Watanabe, J., & Mukai, T. 2006, Abstract, in Proc. 36th COSPAR Sci. Assem., #3145

Brown, P. G., Whitaker, R. W., ReVelle, D. O., & Tagliaferri, E. 2002, Geophys. Res. Lett., 29, 1636

Edwards, W. N., Eaton, D. W., McCausland, P. J., ReVelle, D. O., & Brown, P. G. 2007, J. Geophys. Res., 112, B10306

Fujita, K., et al. 2011, PASJ, 63, 961

Fujiwara, A., et al. 2006, Science, 312, 1330

Ishihara, Y., et al. 2011, Earth Planets Space submitted

Ishihara, Y., Furumoto, M., Sakai, S., & Tsukada, S. 2004, Geophys. Res. Lett., 31, L14702

Ishihara, Y., Tsukada, S., Sakai, S., Hiramatsu, Y., & Furumoto, M. 2003, Earth Planets Space, 55, E9

ReVelle, D. O., Edwards, W., & Sandoral, T. D. 2005, Meteor. Planet. Sci., 40, 895

Spurný, P., Borovička, J., Kac, J., Kalenda, P., Atanackov, J., Kladnik, G., Heinlein, D., & Grau, T. 2010, Meteor. Planet. Sci., 45, 1392

Ueda, M. et al. 2011, PASJ, 63, 947

Watanabe, J., et al. 2011, PASJ, 955

Whipple, F. J. W. 1930, Q. J. R. Meteorol. Soc., 56, 287

Yamaguchi, T., Yoshikawa, M., Yagi, M., & Tholen, D. J. 2011, PASJ, 63, 979

Yamamoto, M.-Y., Toda, M., Higa, Y., Maeda, K., & Watanabe, J. 2005, Earth Moon Planets, 95, 279